SPANDIDOS PUBLICATIONS

Progression of colorectal cancers correlates with overexpression and loss of polarization of expression of the h*tid-1* tumor suppressor

URSULA KURZIK-DUMKE[1], MANUELA HÖRNER[1], JOACHIM CZAJA[1], MARIA RITA NICOTRA[2], NEKTARIA SIMIANTONAKI[3], MICHAEL KOSLOWSKI[4] and PIER GIORGIO NATALI[5]

[1]Institute of Medical Microbiology and Hygiene, Comparative Tumor Biology Group, Faculty of Medicine, Johannes Gutenberg University, Obere Zahlbacher Str. 67, 55131 Mainz, Germany; [2]Institute of Molecular Biology and Pathology, CNR, 11258 Rome, Italy; [3]Institute of Pathology, Johannes Gutenberg University, Langenbeckstrasse 1, 55131 Mainz; [4]Department of Internal Medicine III, Johannes Gutenberg University, Obere Zahlbacher Str. 63, 55131 Mainz, Germany; [5]Regina Elena Cancer Institute, CRS, Immunology Laboratory, Via Delle Messi D'Oro 156, 00158 Rome, Italy

Received July 16, 2007; Accepted August 22, 2007

Abstract. Recently, we identified h*tid-1*, the human counterpart of the *Drosophila* tumor suppressor gene *lethal(2)tumorous imaginal discs* [*l(2)tid*], as a direct molecular ligand of the *adenomatous polyposis coli* (*APC*) tumor suppressor. The gene encodes three cytosolic (Tid50, Tid48 and Tid46) and three mitochondrial (Tid43, Tid40 and Tid38) proteins. In the colorectal epithelium the cytosolic forms hTid50/hTid48 interact under physiological conditions with the N-terminal region of APC. This complex which associates with additional proteins such as Hsp70, Hsc70, Actin, Dvl and Axin defines a novel physiological state of APC unrelated to ß-catenin degradation. Here we show that the expression of the genes h*tid-1* and *APC* was altered in colorectal tumors. These changes concerned both the localization and the expression level of all three h*tid-1* splice variants and of *APC*. Furthermore, we showed that the protein products of the two tumor suppressors co-localized in the basal and apical region of normal colon epithelia and that loss of differentiation capacity of colorectal cancers correlated with a shift in their expression patterns from compartmentalized to diffuse cytoplasmic. These findings support our hypothesis that the building of the multi-component complex mentioned above is associated with the maintenance of the polarity of cells and tissues. In addition, we provide evidence that colon cancer progression correlates with up-regulation of h*tid-1* and its ligand Hsp70. Since the Tid proteins are members of the DnaJ-like protein family, an essential component of the Hsp70/Hsc70 chaperone machinery, our findings describe a novel, causal link between the function of chaperone machines, APC-mediated Wg/Wnt signaling and tumor development.

Correspondence to: Dr Ursula Kurzik-Dumke, Institute of Medical Microbiology and Hygiene, Comparative Tumor Biology Group, Faculty of Medicine, Johannes Gutenberg University, Obere Zahlbacher Str. 67, 55131 Mainz, Germany
E-mail: kurzik@mail.uni-mainz.de

Key words: h*tid-1* tumor suppressor, DnaJ-like co-chaperone, Hsp70 chaperone machinery, Wingless/Wnt signaling, *APC* tumor suppressor, colorectal cancer progression

Introduction

The evolutionarily conserved gene *lethal(2)tumorous imaginal discs* [*l(2)tid*, here below named d*tid*] was originally identified in the fruit fly *Drosophila melanogaster* (1,2). The latter, powerful 'co-worker' of developmental biologists for nearly a century, has also been recognized as an excellent model for human cancer biologists in the last decades (3). The reason why this fly can make a fundamental contribution to identifying and elucidating the functions and functional relationships of human genes causally related to cancer are the biological properties of the epithelial integumental primordia of the fly's adult organs called imaginal discs (4-6). Their growth is regulated by a variety of genes organized in interconnected networks responsible for establishment of cell polarity, pattern formation, direct cell-cell interactions, and extra/intracellular signaling providing cells with information regarding their position in respect to their neighbours, and determining organization and differentiation of tissues (7-9). Interestingly enough, recessive-lethal mutations in these genes have been identified to cause either hyperplastic or neoplastic growth of the imaginal discs (3,10).

The causality of d*tid* in the autonomous but non-invasive growth of the imaginal discs of *Drosophila* was confirmed by gene therapy, performed via P-element-mediated introduction of the wild-type copy of the gene into the germ line, rescuing

the tumor phenotype (2). The mutational events responsible for the tumorous growth were identified (11). Furthermore, we found that the tumor arises from a defined area of the imaginal discs, namely those cells which are responsive to the signaling molecule Hedgehog (Hh) (12). The involvement of d*tid* in the Hh-mediated signaling is mediated by binding of the cytosolic Tid47 protein to the Hh-bound Patched (Ptc) receptor (12).

H*tid-1*, the human counterpart of d*tid*, was isolated by yeast two-hybrid screening as a molecular partner of diverse tumor-related proteins such as the E7 oncoprotein (13), the human interferon-γ receptor subunit R2 (IFN-γR2) (14), the oncogenic viral Tax protein encoded by the human T cell leukemia virus type 1 (HTLV-1) (15), the repressor of IκB kinase ß subunit (16), the ErbB-2 receptor tyrosine kinase (17), the Trk receptor kinases (18) and the von Hippel-Lindau tumor suppressor (19). The murine homolog, m*tid-1*, was identified in a yeast two-hybrid screen as ligand of the Ras GTPase activating protein (GAP) (20). The rat counterpart, rTid, was isolated as a molecular partner of the heat-shock-cognate-glucose-regulated hscGRP75 molecule (21).

H*tid-1* encodes three splice forms h*tid-L*, h*tid-I* and h*tid-S* encoding three cytosolic (hTid50, hTid48 and hTid46 and three mitochondrial (hTid43, hTid40 and hTid38) proteins (22,23). Recently, we identified the cytosolic hTid50/hTid48 molecules as direct molecular partners of the *adenomatous polyposis coli* (*APC*) tumor suppressor (22), a central component of the Wingless(Wg)/Wnt transduction cascade which is directly dependent on Hh-Ptc signaling. Both signaling pathways in question are related to a variety of tumors including colorectal cancer and basal cell carcinoma (BCC) (24-28). As described previously, in BCCs, loss of h*tid-1* correlates with loss of differentiation capacity of the neoplastic cells similar to what was found in the *Drosophila* tumor model (12). Generally, our data suggest that in the case of both ligands Ptc and APC interaction with the Tid proteins maintains their homeostasis essential for proper regulation of proliferation versus differentiation processes of tissues in time and space (12,22).

The present study concerns our identification of hTid50/hTid48 as a direct physiological ligand of APC (22). Here, we described the expression profiles of these two tumor suppressors in normal human colonic epithelium and in poorly, medium- and well-differentiated colorectal cancers. We presented data implicating a clear consistency between the loss of differentiation capacity of the tumors and a shift in degree and subcellular expression patterns of the two proteins. This finding strongly supports our hypothesis linking the binding of hTid50/hTid48 with APC to the cytoskeleton and the establishment of epithelial cell polarity (22). We further showed that the expression level of the DnaJ-like Tid proteins increased in metastases as compared to the primary tumor, thus, suggesting that h*tid-1* up-regulation correlates with tumor progression. Furthermore, we showed that the changes in the expression level of the Tid proteins were accompanied by delocalization and elevated expression of the heat shock protein 70 (Hsp70). This finding is congruent with the functional dependence of the latter on binding to DnaJ proteins acting as their co-chaperones in the Hsp70 chaperone machinery.

Materials and methods

Patient and tissue collection. The normal and tumor surgical biopsies used in this study originated from patients free from therapy undergoing surgical treatment at two institutions: the Regina Elena Cancer Institute, Rome, Italy (33 patients) and the Institute of Pathology, Johannes Gutenberg University, Mainz, Germany (54 patients). Normal epithelium was isolated by microdissection. The patients released informed consent for the experimental use of the specimens. Upon removal, tissue samples were divided into two parts. One part was processed for routine histopathological examination, and the other was immediately shock frozen and stored in liquid nitrogen until investigation. The histological diagnosis followed the criteria of the International Union Against Cancer UICC (29). All samples were characterized according to their TNM and G status. The differentiation state of the specimens originating from Regina Elena Cancer Institute used for immunohistochemistry was determined as poor (10 cases), medium (10 cases) and well differentiated (13 cases) (cf. Results, Table V).

RNA isolation, RT-PCR, and quantitative real-time RT-PCR. Total cellular RNA was extracted from frozen tissue specimens using RNeasy Mini kit (Qiagen), primed with a dT_{18} oligonucleotide and reverse-transcribed with Superscript II (Invitrogen) in accordance with the manufacturer's instructions. The integrity of the obtained cDNA was tested by amplification of p53 transcripts in a 30-cycle PCR at 67˚C using the primers 5'-CGT GAG CGC TTC GAG ATG TCC G-3' (sense) and 5'-CCT AAC CAG CTG CCC AAC TGT AG-3' (antisense). For end point RT-PCR analysis of individual transcripts, 0.5 μl first-strand cDNA was amplified using the QuantiTect SYBR-Green PCR kit (Qiagen), transcript-specific oligonucleotides (300 nM each) and 1 U HotStarTaq DNA polymerase (Qiagen) in a 30-μl reaction volume, 40 cycles, in accordance with the manufacturer's instructions. Each PCR reaction was performed in triplicate using the following reaction conditions: initial denaturation/activation for 15 min at 95˚C, 30 sec at 94˚C, 30 sec of annealing, and 30 sec at 72˚C. In each experiment, a template-free negative control was included. The primer combinations and the annealing temperatures used for the specific amplification of fragments defining the single h*tid-1* splice variants are listed in Table I. Their location in relation to the h*tid-1* sequence (23) is schematically illustrated in Fig. 1. For the specific amplification of an *APC* (30) fragment encompassing nt 10374-10558 the primers 5'-GAT AGG AGT GAA TAC ACC TAC-3' (sense) and 3'-GTA GAC ACA GTA CAG GCA TTG-5' (antisense) were used at an annealing temperature of 60˚C. The relative expression level of specific transcripts was calculated with respect to the internal standard (= reference) hypoxanthine guanine phosphoribosyl transferase (HGPRT) used to standardize each reaction run with respect to RNA integrity, sample loading and inter-PCR variations. Amplification of HGPRT was performed using the primers 5'-TGA CAC TGG CAA AAC AAT GCA-3' (sense) and 5'-GGT CCT TTT CAC CAG CAA GCT-3' (antisense) at an annealing temperature of 62˚C. A template-free negative control was included in each experiment.

Primer combinations used to amplify the h*tid-1* splice variants h*tid-L*, h*tid-I* and h*tid-S*.

Splice form	5' primer designation, sequence, location, region of the gene[a] (nt)	3' primer designation, sequence location, region of the gene[a] (nt)	Annealing temperature/ size of the amplified fragment (nt)
h*tid-L* exon 1-11	P1f GTTGACATTCAATCAAGCTGC exon 5, 642-662	P1r CTGGGATATCATGAGGTAAAC exon 11, 1451-1431	58˚C/812
h*tid-I* exon 1-10 and 12	P1f GTTGACATTCAATCAAGCTGC exon 5, 642-662	P2r CCAGTGGATCTTTTT**C**CAGAG exon 12/10, 1472-1458/**1340**-1335	62˚C/716
h*tid-S* exon 1-4 and 6-12	P3f CAGCCTCAGGAA**G**AAACCATC exon 4/6, 619-630/**784**-792	P3r GGGAT**C**GTCACGTTGATCGTC exon 9/8, 1131-1126/**1125**-1110	54˚C/339

P, primer; f, forward; r, reverse; [a]The nt positions are congruent to the sequence published by Yin and Rozakis-Adcock (cf. Fig. 1) (23). In those cases where the used primers encompass two exons, the position of the first nucleotide of the second exon is in bold print and underlined.

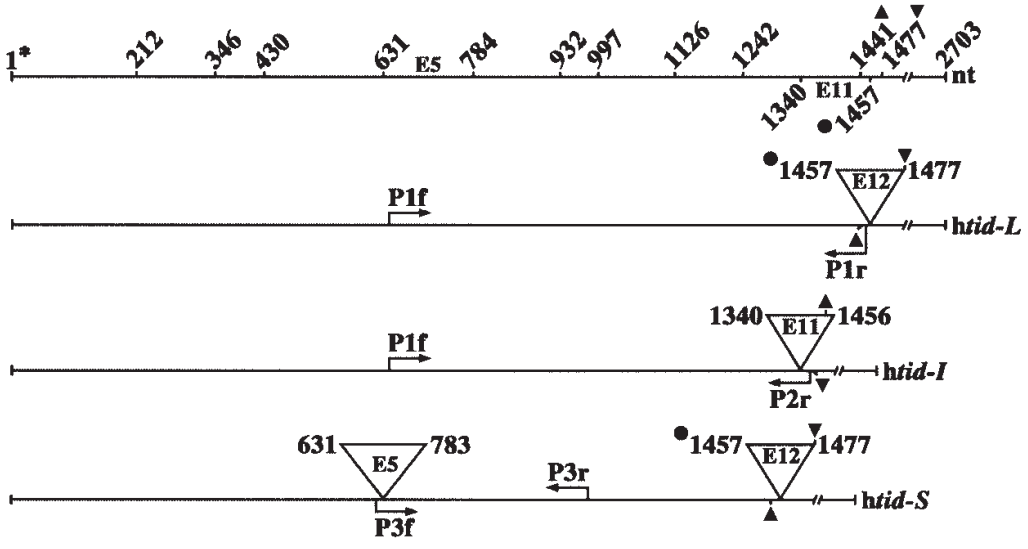

Figure 1. Schematic illustration of the location of the primers used for amplification of the h*tid-1* splice variants *L*, *I* and *S* in relation to the length of the protein coding region of the gene (23). h*tid-L* consists of exons 1-11; h*tid-I* is build of exons 1-10 and 12; and h*tid-S* is generated by alternative splicing of exons 1-4 and 6-11 (cf. Table II). In the upper scale, the nt positions of the first nucleotide of each exon are given. 1* marks adenine (A) of the start codon. The sequences of the primers are listed in Table I. f, forward; r, reverse.

Quantitative real-time RT-PCR analysis was performed using the ABI PRISM 7300 Sequence Detection System instrument and software (Applied Biosystems). In this approach, the fluorescent dye SYBR-Green was used to monitor DNA synthesis. We measured the cycle number at which the fluorescence intensity was greater than the background fluorescence; thus, at which the target amplification was first detected. This value is referred to as the cycle threshold, the Ct value. Consequently, the greater the DNA quantity of the target in the starting sample, the faster a significant increase in fluorescence signal will appear, yielding a lower Ct. During the exponential phase of the PCR with 100% efficiency (E) of the reaction, the fluorescence doubles at each cycle (factor 2 in the efficiency formula below) in accordance with doubling of the amount of the amplicon. The Ct value is proportional to the logarithm of the initial amount of the target DNA in the sample. Thus, the relative concentration of one target with respect to another is reflected in the difference in the cycle number, the ΔCt value, which is necessary to achieve the same level of fluorescence. In this study the differences in the Ct values between the target gene/splice form of interest (X) and the reference (R, here HGPRT) are referred to as ΔCt values and were calculated as follows: ΔCt(X) = Ct(X) - Ct(R). A ΔCt of 0

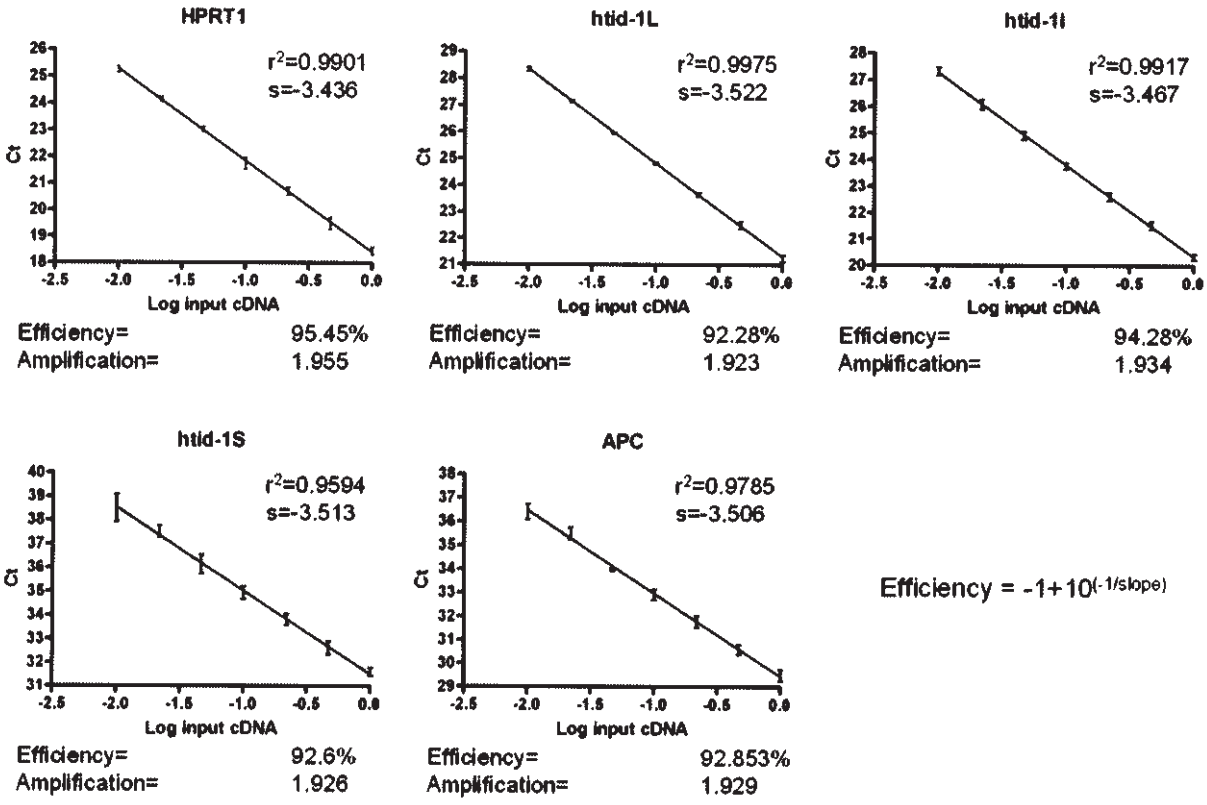

Figure 2. Determination of real-time PCR efficiencies of the reference gene HGPRT (HPRT1) and the target tumor suppressor genes h*tid-1* and *APC*. The cycle numbers (cycle threshold, Ct) necessary to achieve the given level of fluorescence versus cDNA (reverse-transcribed total RNA) concentration input were plotted to calculate the slope (s) (mean ± SD, n=3). Regressions were calculated using the graphad prism software. The corresponding real-time PCR efficiencies (E) were calculated according to the equation $E = 10^{(-1/slope)}$. r^2, coefficient of determination.

indicates a ratio of 1 between the target and the reference [$2^{-(\Delta Ct)} = 2^0 = 1$; the number 2 defines the doubling of the amount of the amplicon with each reaction by 100% E]. Since E is determined by factors such as optimal design of primers, real-time PCR conditions, we previously optimized it for each target gene investigated (Fig. 2). Regressions were calculated using the graphad prism software. The Ct values versus cDNA (reverse-transcribed total RNA) concentration input were plotted to calculate the slope (mean ± SD). The corresponding real-time PCR efficiencies were calculated using the equation: $E = 10^{(-1/slope)}$. After normalization of the Ct values of both tumor and normal samples with respect to HGPRT, the change $\Delta\Delta Ct$ in the expression levels of the target transcripts in the tumor sample as compared to normal tissue was calculated as follows: $\Delta\Delta Ct = \Delta Ct_{tumor\ sample} - \Delta Ct_{normal\ sample}$.

Western blot analysis. The normal and tumor surgical biopsies used for Western blotting originated from patients free from therapy and undergoing surgical treatment at the Institute of Pathology in Mainz. Crude protein homogenates were prepared using a Dounce homogenizer in ice-cold TKM buffer (50 mM Tris, pH 7.5/150 mM KCl/5 mM $MgCl_2$) supplemented with the Protease Inhibitor Cocktail Complete™ (Boehringer) to a final concentration of 1 mM. All operations were performed at 4˚C. The total protein amount was quantified using the Bio-Rad Protein Assay (Bio-Rad Laboratories GmbH). The anti-hTid$^{66-480}$ antibodies (Abs) (cf. Antibodies) were used in a dilution 2 μg/ml in TBS blocking buffer (0.05 M Tris/0.15 M NaCl, pH 7.5) containing 3% BSA (Sigma). All other Abs (cf. Antibodies) applied for immunodetection by Western blotting were used at the highest concentrations recommended by the manufacturer. Proteins were visualized using appropriate secondary AP-linked Abs or by enhanced chemiluminescence using the BM Chemiluminescence Western Blotting Kit in accordance with the manufacturer's instructions (Chemikon).

Antibodies. In order to detect the Tid proteins, we generated a polyclonal rabbit antibody, anti-hTid$^{66-480}$, against the recombinant hTid protein fragment corresponding to amino acids (aa) 66-480 as described previously (22). Booster injections, purification of antisera and determination of concentration via ELISA were performed as described previously (11,12). The mAbs against APC (F-3), the polyclonal rabbit Abs against APC H-290 and C-20 were purchased from Santa Cruz Biotechnology, Inc. The mAb against E-Cadherin (clone 5H9) was purchased from Progen. Mouse and rat mAbs to Hsp70 (SPA-819) and Hsc70 (SPA 815) were purchased from Biomol. Rabbit polyclonal serum against the C-terminus of Actin was obtained from Sigma. Secondary Abs labeled either with FITC or Cy3 were acquired from Sigma.

Immunohistochemistry. For immunohistochemistry of the samples originating from Regina Elena Cancer Institute (cf.

TNM status and grading of the human colon adenocarcinomas investigated.

Sample	1	2	3	4	5	6	7	8	9
T	2	3	3	3	3	3	3	3	3
N	0	0	0	0	2	2	2	2	2
M	no	no	no	no	no	no	no	no	no
G	2	2	2	2	2	2	2	1-2	2-3
Sample	10	11	12	13	14	15	16	17	18
T	x	2	3	3	4	4	3	x	x
N	x	2	1	2	1	2	2	x	x
M	no	no	no	no	no	no	yes	yes	yes
G	x	3	3	3	3	3	3	x	x

T, tumor extension: T1, to submucosa; T2, to muscle layer; T3, to subserosa; T4, to serosa. N, lymph node affection; M, metastasis. G, grading: G1, well differentiated; G2, medium differentiated; G3, undifferentiated; x, not defined.

Patient and tissue collection), 4-μm cryosections were fixed in cold absolute acetone for 10 min. Biopsies were stained with the affinity purified polyclonal rabbit anti-hTid$^{66-480}$ Abs at the concentration of 40 μg/ml and the polyclonal rabbit Abs to the N-terminus of APC (H-290) (Santa Cruz) at the concentration of 20 μg/ml. Avidin-biotin indirect immunoperoxidase staining was carried out in accordance with standard procedures using commercially available reagents (Vectastain Elite). Sections incubated with normal rabbit IgG served as negative controls. 3-amino-9-ethylcarbazole (Sigma) was used as a substrate for horseradish peroxidase. Sections were counterstained with Mayer's hematoxylin. Three non-consecutive sections of each biopsy, representative of different areas of the tumor, were analyzed. Indirect immunofluorescence studies were carried out on the same substrates employing the polyclonal rabbit anti-hTid$^{66-480}$ Abs (see above) and a mouse monoclonal Ab (mAb) to APC (clone ALI 12-28, 10 μg/ml) purchased from Upstate. Fluorescein (FITC)-labeled goat anti-rabbit Ig (Cappel Labor West) and Texas-Red-labeled rabbit anti-mouse Ig (Molecular Probes) were used as secondary Abs. Slides were mounted with DAPI containing mounting medium (Vector) and observed using a light and a Leica confocal microscope (Leica). Biopsies originating from patients undergoing surgical treatment at the Institute of Pathology in Mainz (cf. Patient and tissue collection) were formalin (4%)-fixed and paraffin-embedded in accordance with standard procedures. Sections (3-μm) were used for immunostaining reactions performed using the avidin-biotin/horseradish peroxidase complex (ABC/HRP) (Vectastain Elite) in accordance with standard protocol (31). Prior to the blocking of the non-specific background, sections were incubated 15 min in a commercial microwave oven (600 W) and then cooled for ~20 min at room temperature. The samples were stained using anti-hTid$^{66-480}$ and the mAbs against Hsp70 and Hsc70 (cf. Antibodies).

Statistical examination. RNA expression levels were reported as the mean values (n=3) ± standard deviation (SD). Statistical evaluation was performed using the Student's t-test.

Results

The expression of RNA encoded by the tumor suppressors htid-1 and APC was altered in human colorectal cancers. H*tid-1* is composed of 12 exons separated by 11 introns (23). It encodes three splice variants, h*tid-L*, h*tid-I* and h*tid-S* generated by alternative splicing of exons 5 (153 nt), 11 (99 nt) and 12 (18 nt) of the gene (22,23). H*tid-L* consists of exons 1-11 (Fig. 1). The h*tid-1* I form consists of exons 1-10 and exon 12, and the h*tid-1* S form of exons 1-4 and 6-11 (Fig. 1; Table I). As described previously, h*tid-1* expression is tissue and developmental stage specific (22). In tissues of the human gastrointestinal tract such as the stomach, jejunum, ileum, colon and rectum, transcripts corresponding to all three splice variants were detected (22). To examine whether the expression of the single h*tid-1* splice variants differed in colorectal cancer as compared to normal colon epithelium, real-time PCR analysis of 18 adenocarcinomas of the colon, characterized with respect to the TNM and G status (Table II), was performed (Table III). The expression levels determined in colorectal cancers (Table III) were established in relation to an average expression profile defined for normal samples as 100% (Table IV). With respect to the expression levels of the h*tid-1* splice variants in normal tissue, the Ct values (cf. Materials and methods) shown in Table IV described the highest expression for the I form and the lowest for the S form. This profile is consistent with data on expression of the hTid proteins (22) (Fig. 3A, h). As shown in Table III, all tumors investigated expressed aberrant RNA profiles of both tumor suppressors, h*tid-1* and *APC*, as compared to normal tissue. In the case of h*tid-1,* the differences concerned all three splice variants. The h*tid-1* expression patterns varied from down- (cases 1, 2, 6, 11-13, 15, 17 and 18) to up- (cases 3, 4, 9 and 10) regulation of all three forms. Interestingly enough, in the latter 4 cases the increase of h*tid-L* expression was clearly higher as compared to the other two splice variants. In two cases (8 and 14) a prominent up-regulation of h*tid-L* was detectable whereas the two smaller forms were down-regulated. Generally, the h*tid-1* RNA levels detected in

Table III. Percentage of increase/decrease of expression of the three h*tid-1* splice forms *L*, *I* and *S*, and *APC* in human colon adenocarcinomas as compared to normal tissue (100%).

Sample	1	2	3	4	5	6	7	8	9
h*tid-L*	28	53	611	516	637	37	94	250	1136
h*tid-I*	26	70	114	139	146	11	102	64	252
h*tid-S*	42	89	114	102	44	3	98	26	165
APC	14	80	5	14	55	23	39	5	49
Sample	10	11	12	13	14	15	16	17	18
h*tid-L*	704	37	46	23	240	66	71	41	33
h*tid-I*	180	45	60	35	54	64	147	66	45
h*tid-S*	208	19	55	6	8	51	177	63	63
APC	84	26	11	34	24	13	16	69	85

The expression levels were calculated as follows: $\Delta\Delta Ct = \Delta Ct_{tumor\ sample} - \Delta Ct_{normal\ sample} \times 100\%$ (cf. Table IV and Materials and methods). The designation of the samples (1-18) corresponds to that described in Table II.

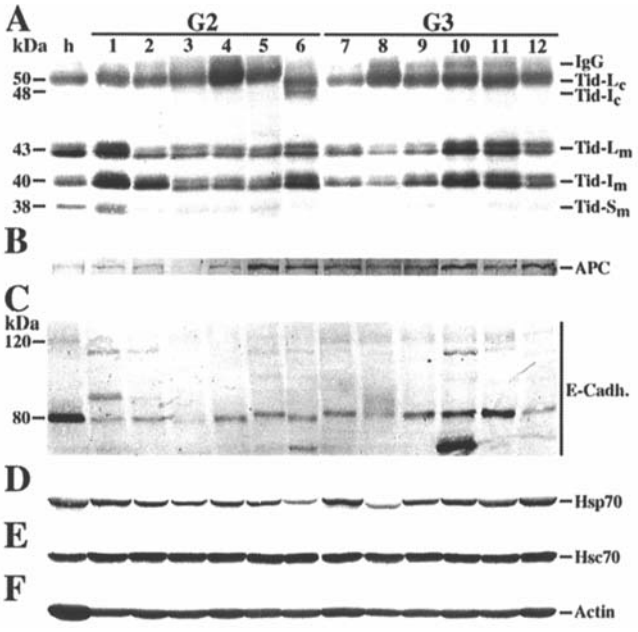

Figure 3. Immunoblot of crude homogenates from normal colon epithelium (h) and colorectal cancers (1-12) stained using anti-hTid$^{66-480}$ (A), anti-APC (B), anti-E-Cadherin (C) anti-Hsp70 (D), anti-Hsc70 (E) and anti-Actin (F). The expression level in the normal sample h represents an average expression profile. The homogenate was generated from a pool of normal colon epithelium derived from 5 patients. G, grading.

the tumor samples did not indicate an association with either the TNM or the G status of the samples.

With regard to APC, all tumor cases investigated showed lower RNA levels as compared to normal tissue (Table III). In most cases (1, 3, 4, 8, 11, 13 and 16), the expression decreased below 20% of that determined in normal epithelium. Similar to the values determined for the h*tid-1* splice variants, the results obtained for *APC* indicated no relationship between the RNA expression level and the TNM and/or G status of the examined samples.

Primary colorectal tumors express aberrant levels of the distinct Tid proteins and APC. By Western blot analysis of immunoprecipitates performed from normal colon epithelia and from subcellular fractions isolated by differential centrifugation and separation on continuous sucrose gradients, three cytosolic (hTid50, hTid48 and hTid46) and three mitochondrial (hTid43, hTid40 and hTid38) proteins were identified (22). Furthermore, this analysis revealed that the mitochondrial proteins L and I occur in two forms postulated to be posttranslational modifications (22). Whereas all three mitochondrial forms were well visible in crude homogenates (Fig. 3A, h), the cytosolic forms I and S were detectable under normal conditions first after enrichment by immunoprecipitation (22). In primary colorectal cancers, G2 (Fig. 3A, cases 1-6) as well as G3 (Fig. 3A, cases 7-12), the expression profiles of the Tid proteins differed as compared to normal colon epithelia (Fig. 3A, h). The differences concerned both their expression levels and the ratio of the two forms postulated to be posttranslational modifications (22). The S form was either very weakly expressed or not detectable (Fig. 3A). Similarly, as established using quantitative real-time RT-PCR (Table III) in most of the cases de-regulation of more than one of the Tid proteins was detectable (Fig. 3A). A relationship between the expression levels of either of the Tid proteins generally or a defined Tid form and the differentiation stage of the tumor could not be established at present.

Because of the physiological interaction of the products of the tumor suppressors h*tid-1* and *APC* (22) and because of the fact that the Tid proteins as members of the DnaJ class of molecular co-chaperones are functionally linked with the Hsp70/Hsc70 proteins (32), we examined the above tumor samples for the expression of APC, Hsp70 and Hsc70. As shown in Fig. 3B, APC was expressed in all samples. Furthermore, since the Abs used for this study, APC (C-20), are directed against the C-terminal part of the molecule, the results obtained suggest that the detected bands corresponded to the full-length APC molecule (Fig. 3B). Generally, in most

ΔCt values determined in normal colon epithelium for the tumor suppressors h*tid-1* and *APC* by real-time PCR.

Target gene/splice variant	h*tid-L*	h*tid-I*	h*tid-S*	*APC*
Samples/ΔCt value	4.84	2.10	16.120	9.35
	3.56	1.40	13.465	9.64
	4.81	1.90	15.145	9.76
	4.39	1.78	15.000	
	4.17	1.54	13.920	
ΔCt (%)	4.36 (100)	1.74 (100)	14.73 (100)	9.58 (100)
$\frac{1}{n}\sum \chi - \bar{\chi}$	±0.38	±0.22	±0.83	±0.83

ΔCt = Ct (target gene) - Ct (HGPRT); $\frac{1}{n}\sum \chi - \bar{\chi}$: Standard deviation (SD); n=3.

of the G2 tumors (cases 1-4) its expression was comparable to that detected in normal epithelium (Fig. 3A, cases 1-4, cf. h) whereas G3 tumors exhibited definitely higher APC levels as normal tissue (Fig. 3B, lanes 7-12, cf. h). These results were not consistent with the real-time PCR data. They suggested that the development/progression of the adenocarcinomas investigated by real-time PCR and by Western blot analysis may be due to aberration of further colon cancer-related molecules, components of the Wnt/Wg pathway, e.g. E-Cadherin (27,32,33). Indeed, determination of E-Cadherin expression in these samples revealed that the full-length 120-kDa molecule was, in all the cases investigated, either degraded or its level of expression was altered (Fig. 3C). Furthermore, some cases were characterized by very low expression levels of both the 120-kDa and 80-kDa molecule. In some cases the 80-kDa E-Cadherin molecule was also degraded. Thus, generally, the samples investigated by Western blotting were all characterized by aberrant expression profiles of E-Cadherin as compared to normal tissue.

With respect to Hsp70 (Fig. 3D) the primary cancers showed differences in its expression levels as compared to normal epithelium. However, a correlation between up-regulation of Hsp70 and tumor progression as detected by immunohistochemistry of primary cancers and metastases (cf. Fig. 4, E-H) was not prominent between the G2 and G3 tumors. In contrast, the expression of Hsc70 was comparable for the normal tissue and the primary tumors (Fig. 3E). The similar Actin (control for loading) expression levels detected in all tumor samples (Fig. 3F) indicated that the experimental conditions were well standardized. The higher Actin level detected in the normal epithelium as compared to tumor samples is consistent with the fact that tumors are generally characterized by down-regulation of the Actin system (34).

The pattern of the anti-hTid$^{66\text{-}480}$ and anti-APC stain changes in primary tumors from compartmentalized to homogenous in accordance with loss of differentiation capacity. The analysis of colorectal tumors by real-time PCR and Western blot analysis (Tables II-V; Fig. 3A and B) showed that the expression profiles of the functionally linked tumor suppressors h*tid-1* and *APC* were altered in primary colorectal cancers. These data concern the general expression levels of the two genes. However, they do not provide information regarding the distribution of the products of the genes at the cellular level. Thus, to elucidate the possible link between the changes in the expression profiles of the two genes and the tumorigenic process, we next examined their expression profiles in colorectal cancers by immunohistochemistry. This analysis was performed using different tissue substrates namely cryosections originating from the Regina Elena Cancer Institute in Rome (Table V; Fig. 4) and formalin-fixed paraffin-embedded biopsies originating from the Institute of Pathology in Mainz (Fig. 5). The former samples were classified according to their differentiation state into three groups: well (13 cases), medium (10 cases) and poorly differentiated (10 cases) (Table V; Fig. 4). The expression patterns were detected using fluorescence (Fig. 4A-F) and light microscopy (Fig. 4G-J). As shown in Fig. 4A, in the normal human colon, the h*tid-1* expression was limited to the epithelium. Here staining performed using the anti-hTid$^{66\text{-}480}$ Abs was visible from the crypt up to the luminal area in the basal (arrowheads), apical (triangles) and the lateral (arrows) cytoplasm (Fig. 4A, C and D), but not in the apical-luminal area. APC was expressed in the epithelium (Fig. 4B-D). Here the Abs against APC used stained the basal (arrowheads), lateral (arrows), apical (triangles) and apical-luminal parts (stern, cf. Fig. 4C and D, the red rim underneath the region where the molecules in question co-localized in the apical area). Thus, the distribution of both tumor suppressors in question was closely associated with the pronounced apical-basal polarity of epithelial cells. As shown in Table V and Fig. 4, the pattern of the anti-hTid$^{66\text{-}480}$ stain changed from compartmentalized to homogenous (Fig. 4E-G and I) in accordance with loss of differentiation capacity of the tumors. The normal distribution was already less prominent in the well-differentiated tumors (Fig. 4E and F) where it was visible in most cases either in the basal or apical portion and only rarely at both poles as was the case in normal cells (Fig. 4A, C and D). In fourteen of the 33 cases investigated (42.4%) the immunoreaction was definitely stronger (++) in the entire tumor (Table V, cases 1, 2, 4, 5, 11-15, 17, 21, 23, 25 and 30) as compared to normal epithelium (+). This finding strongly

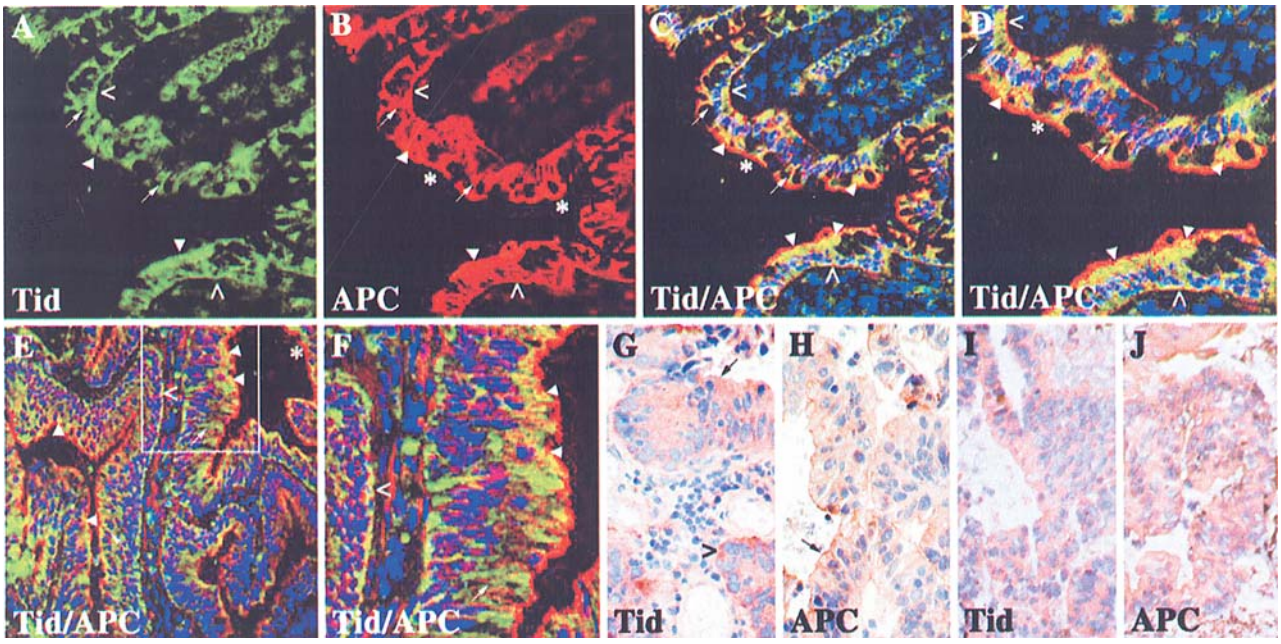

Figure 4. H*tid-1* and *APC* expression is altered in colorectal tumors. Laser scan micrographs of normal (A-D) and well-differentiated colon cancer (E,F) stained using anti-hTid$^{66-480}$ (A,C-F) and anti-APC (clone ALI 12-28) (B,C-F). Anti-hTid$^{66-480}$ stained the basal (arrowheads), lateral (arrows) and the apical (triangles) cytoplasm of the epithelium, from crypts to the luminal area. Anti-APC staining is visible in the basal (arrowheads), lateral (arrows), apical and the apical-luminal (sterns, cf. C,D, the red rim illustrating the presence of APC, but not hTid) cytoplasm. Co-localization is visible in those areas where both proteins are expressed (C-F). In the well-differentiated carcinoma (E,F) the expression pattern of both proteins is already less focused as compared to normal tissue. Light micrographs of medium (G, H) and poorly (I, J) colon cancer stained for hTid (G, I) and APC (H, J). The expression pattern of both hTid and APC changed from compartmentalized to homogenous in accordance with loss of differentiation of the tumors. The arrowhead in G marks the basal area whereas the arrow labels the apical part. The arrowhead in H marks the apical-luminal region.

implicates up-regulation of expression which, however, does not necessarily seem to be associated with a loss of the differentiation state of the tumors. Similarly in the poorly, medium- and well-differentiated cancers, cases showing a weak stain with negative areas, homogenous stains comparable to those found in normal cells and strong stains were found (Table V). The percentage of cases exhibiting a strong stain varied from 30.8% in well-differentiated tumors, 40% in poorly differentiated samples to 60% in medium-differentiated cancers.

The distribution and the expression levels of APC were also altered in the investigated colorectal cancers (Table V). Similar to h*tid-1*, in poorly differentiated cancers, *APC* was no longer compartmentalized, but homogenously distributed (Fig. 4J). In most of the well- and medium-differentiated cancers, the anti-APC staining in the apical region (Fig. 4H) was preserved whereas only isolated areas were stained in the basal portion. In this subset, also staining in the lateral areas was observed (Table V). Generally, in most of the 33 tumors investigated (19 cases), weaker APC expression was visible in the tumor as compared to normal epithelium. This finding is consistent with the data obtained using real-time PCR (Table III). One case of poorly differentiated cancer was negative for h*tid* (Table V, case 3). The same case was also negative for APC. Since, however, in two further APC negative cases, one well (Table V, case 29) and the other medium differentiated (Table V, case 20), the h*tid* level was either comparable to that detected in normal epithelium (Table V, case 29) or weak with negative areas (Table V, case 20), it can only be stated at present that loss of h*tid-1* is not necessarily linked to loss of APC.

The analysis of colorectal cancers by Western blot analysis revealed, furthermore, that h*tid-1* expression was also altered in colorectal cancers characterized by aberrations of E-Cadherin expression profiles (Fig. 3C). As described previously, E-Cadherin is not a direct molecular ligand of the Tid molecules (22). Thus, the aberrant expression profiles of h*tid-1* and E-Cadherin are not a consequence of a functional link.

Increase of htid-1 and hsp70 expression correlates with tumor progression. The correlation between loss of differentiation capacity and loss of compartmentalization of h*tid-1* discussed above concerns primary colorectal tumors. Thus, to investigate the potential association of h*tid-1* expression with tumor progression, we next examined comparatively in 24 colon cancers (12 G2 and 12 G3) the expression levels of the gene in the normal epithelium, in the primary tumor, and in the lymph node and liver metastasis derived from one patient. As shown in Fig. 5, h*tid-1* up-regulation correlated with tumor progression. The intensity of the staining was visibly stronger in the primary tumor (Fig. 5B) as compared to normal tissue (Fig. 5A). The lymphatic infiltration visible in Fig. 5B (arrow) already indicated that up-regulation of h*tid-1* was associated with tumor progression. Anti-hTid$^{66-480}$ staining of the lymph node (Fig. 5C) and liver metastasis (Fig. 5D) supports this finding.

Upon consideration that DnaJ-like proteins act in concert with the Hsp70/Hsc70 molecules whose expression have been found to be altered in a variety of cancers, we examined the same samples for expression of both Hsp70 and Hsc70 (22,35-37). As shown in Fig. 5E, Hsp70 was expressed in the basal and luminal cytoplasm of the normal epithelium. In the

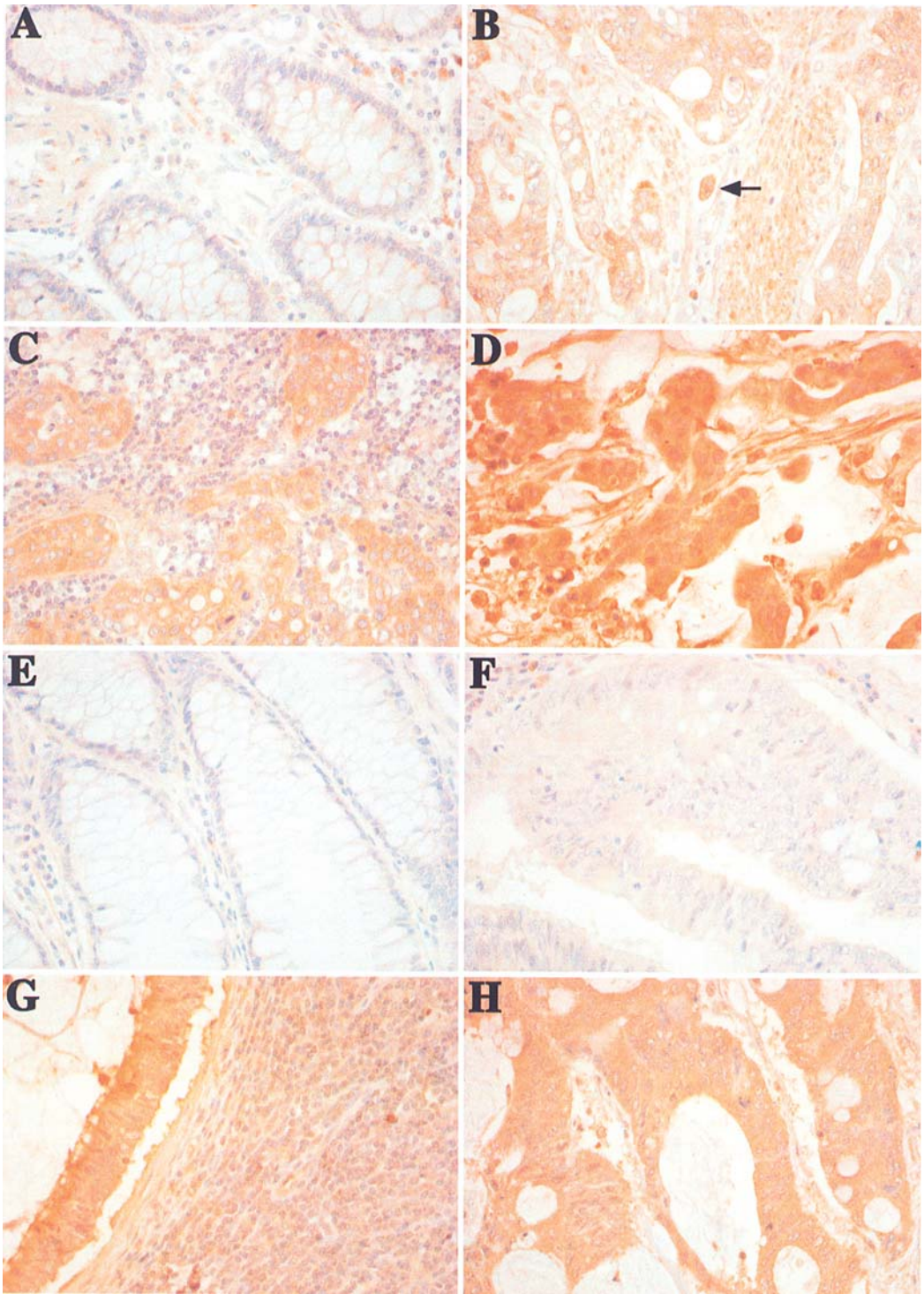

Figure 5. Increase of h*tid-1* (A-D) and Hsp70 (E-H) expression correlates with tumor progression. Anti-hTid$^{66-480}$ staining of normal colon (A), primary tumor (B), lymph node metastasis (C) and liver metastasis (D) derived from one patient. The strong staining of the infiltrate of lymph vessels visible in the primary tumor (B, arrow) indicates that h*tid-1* up-regulation correlates with metastasis. The results of anti-hTid$^{66-480}$ staining of lymph node (C) and liver metastasis (D) support this finding. Hsp70 expression in normal colon (E), primary tumor (F), lymph node metastasis (G) and liver metastasis (H). The sections originate from the same samples as shown in A-D. Note that up-regulation of Hsp70 correlates with tumor progression similarly as shown in A-D for h*tid-1* using anti-hTid$^{66-480}$ for staining.

primary tumor (Fig. 5F) and in lymph node (Fig. 5G) and liver (Fig. 5H) metastases, the level of the protein was clearly increased as compared to the normal epithelium, similarly as detected for h*tid-1* (Fig. 5A-D) in comparable tissue substrates. In contrast, staining of the same tumor samples using anti-Hsc70 showed that loss of polarity and differentiation of the cells did not alter the expression of Hsc70 which was uniformly distributed in the cytoplasm of colon epithelia (data not shown).

Discussion

In recent years the cancerogenous steps of colorectal cancer, the second most common cancer in developed countries, have

Table V. Degree of expression and distribution patterns of Tid and APC in colorectal cancers of varying differentiation grade.

No.	Patients	hTid		APC	
	Poorly differentiated	Intensity	Patterns[a]	Intensity	Patterns[a]
1	ASC	++		±	isolated apical
2	LAB	++		±	isolated apical
3	BRI	-		-	
4	SEN	++		+	
5	SPA	++		±	
6	ART	±		±	
7	ROA	±		±	
8	FLO	+		+	
9	BON	+		+	
10	RAP	±		++	
	Moderately differentiated	Intensity	Patterns	Intensity	Patterns
11	PRA	++		±	apical, isolated latero-lateral
12	QUA	++	basal	+	isolated basal
13	BRA	++	apical, basal	+	apical, isolated latero-lateral
14	MAR	++	apical, basal	±	apical
15	GEN	++	apical, basal	±	isolated apical and latero-lateral
16	FIO	+	isolated basal	±	apical, isolated latero-lateral
17	DIN	++		±	apical, latero-lateral
18	MAG	+		±	
19	CET	±		±	
20	CIA	±		-	isolated apical
	Well differentiated	Intensity	Patterns	Intensity	Patterns
21	DEL	++		±	apical, isolated basal
22	MAN	+	basal	+	apical
23	GRI	++	basal	±	apical, isolated latero-lateral
24	CAS	+	basal	±	apical, isolated latero-lateral
25	LUPS	++	apical, basal	+	apical, isolated latero-lateral
26	DEA	±	apical, basal	±	apical, isolated latero-lateral
27	AVV	+	apical, basal	+	apical, isolated latero-lateral
28	DEA	+	apical, basal	±	apical, isolated latero-lateral
29	POL	+	apical, basal	-	isolated apical
30	DAQ	++	apical	±	
31	FAR	±	apical	±	apical
32	MAL	±	apical	+	apical
33	FIL	+	apical	+	apical

-, no stain; ±, weak stain with negative areas; +, homogenous stain; ++, homogenous strong stain. [a]If not specified, then the cytoplasmic staining pattern does not display a subcellular polarization.

been elucidated considerably. However, important gaps still remain. Our recent discovery of the cytosolic Tid proteins Tid50/Tid48 as direct physiological partners of APC suggests a novel functional relationship of the latter in the already well-established Wg/Wnt signaling related to diverse pathological events, among them colorectal cancer.

Both inherited and sporadic colonic tumors arise sequentially from precancerous polyps or adenomas (38). Colorectal tumorigenesis proceeds through a series of genetic alterations in evolutionarily conserved oncogenes and tumor suppressor genes which in accordance with the model proposed by Vogelstein and co-workers occur in a sequential order and are associated with well-defined morphological changes (39). The progression of the disease is evidently determined by the total accumulation of these events. Some of the genes involved, e.g. APC, act in tumor initiation and progression (39). However, alterations of the function of further components of the Wg/Wnt pathway such as E-Cadherin, ß-Catenin, and GSK-3ß are also causally linked to colorectal and other cancers (9,24,27).

multifunctional APC protein acts in the Wg/Wnt-signal transduction, apoptosis, cell migration and chromosomal segregation at mitosis (24,26-28). The conserved Wg/Wnt signaling plays a critical role in development and oncogenesis (32). It regulates cell fate and pattern formation in invertebrates and vertebrates (3,8,9). Its developmental role has been studied using animal models such as *Drosophila*, *C. elegans* and *Xenopus*. In *Drosophila,* disruption of the signaling causes segment polarity defects (3). In vertebrates, mutations affecting the function of the various genes participating in the cascade, acting either as tumor suppressors or oncogenes, are causal in the development of a variety of cancers (9,24,27). The functional analysis of these genes performed using the above mentioned animal systems and mammals allowed the establishment of the canonical Wg/Wnt signaling currently known. It plays alternative roles in cell migration and adhesion. In the presence of the signaling molecule Wg/Wnt, the cascade is activated and regulates the level of ß-Catenin accumulating in a complex with TCF/LEF transcription factors driving expression of target genes such as c-myc or cyclin D1 involved in the regulation of cell proliferation (26-28).

The direct link between loss of the d*tid* gene function(s) and tumor formation has been definitely documented by germ line rescue of the *Drosophila* tumor phenotype (12). Its isolation as a molecular ligand of oncogenes, tumor suppressors and other cancer-related molecules supports its causal involvement in tumor onset via different modes (12-22). Our recent identification of Tid50/Tid48 as APC partner (22) extends the list of its tumor-related physiological ligands and, furthermore, provides additional proof for its action at different levels of cancer-related signaling networks. Therefore, loss of function and/or malfunction of h*tid-1*, may affect diverse physiological events and, vice versa, its action may be affected by de-regulation of various genes. Indeed, our preliminary study on h*tid-1* expression in various cancers showed alteration of its expression in diverse cancers (40).

In this study we provide clear evidence that h*tid-1* is altered in colorectal carcinomas. These alterations were linked to both loss of polarity of the cancer cells and tumor progression. In normal colon epithelium, the distribution of both tumor suppressors h*tid-1* and *APC* was closely associated with the pronounced apical-basal polarity of epithelial cells. In colorectal cancers, h*tid-1* expression was altered with respect to both the levels of expression and distribution. The concordance of h*tid-1* up-regulation with tumor progression suggests that the physiological level of h*tid-1* expression is associated with negative regulation of the proliferative potential of the epithelial cells. The alterations of h*tid-1* RNA levels concerned all three splice variants of the gene and varied from down- to up-regulation of the single forms. Since altered h*tid-1* levels were detectable in all colon carcinomas (a total of 57 cases were investigated by immunohistochemistry, 18 cases by real-time PCR and 12 cases by Western blot analysis), as well as those which showed decreased APC levels and those which were characterized by alterations of E-Cadherin expression profiles, this phenomenon seems to be of general relevance to colon cancer. However, in the case of APC, the direct ligand of the cytosolic hTid50/hTid48 molecules, the prominent changes in h*tid-1* profiles were accompanied by changes in the distribution of APC. Generally, the h*tid-1* and APC RNA levels detected in the investigated tumors did not indicate an association with either the TNM and/or the G status of the samples. However, already in primary tumors the distribution of both tumor suppressors changed from compartmentalized to homogenous in accordance with loss of polarity and differentiation capacity of the epithelial cancer cells. This finding is consistent with the role of APC in maintaining the apical-basal polarity of the colonic epithelium. It is also in keeping with our previously published hypothesis that the binding of Tid to APC is associated with maintaining the distinct roles of APC in the cancer-related Wg/Wnt signaling and regulating the onset of proliferation of cells (22).

With respect to the association of h*tid-1* with the metastatic potential of colorectal tumors, an increase in h*tid-1* level was already visible in infiltrates of lymph vessels in primary tumors. Metastases, such as lymph node and liver, showed drastic up-regulation of h*tid-1*. Interestingly enough, these changes were accompanied by up-regulation of Hsp70, a direct ligand of the DnaJ-like hTid50/hTid48 molecules and their partner in building the multi-component complex consisting of Tid50/Tid48-bound APC, Hsp70, Hsc70, Actin, Dvl and Axin (22). Thus, these findings provide additional support to our previously published hypothesis that h*tid-1* function is crucial at distinct levels of cancer-related signaling networks involved in the regulation of cell polarity and fate and pattern formation and is related to both neoplastic transformation of cells and cancer progression (12,22).

As described previously the Tid proteins belong to the DnaJ co-chaperone family functionally linked to the evolutionarily conserved Hsp70/Hsc70 chaperone machinery responsible for correct folding and assembly/disassembly of proteins and protein complexes (35,36). In higher eukaryotes this machinery orchestrates a variety of processes determining both embryonic and the entire adult life. Furthermore, its association with tumorigenic processes has been well documented (37).

Our identification of APC as a molecular ligand of hTid50/hTid48 and, furthermore, in a complex with Hsp70/Hsc70, Actin, Dvl and Axin presents a novel aspect concerning the biology of cancers associated with either loss or malfunction of APC (22). Namely, the malfunction of APC does not necessarily result from the alteration in the *APC* gene itself, but may go along with changes in h*tid-1* function or even results from it. Furthermore, aberration in expression of the hTid proteins determining the function of the Hsp70/Hsc70 molecules may go along with changes in the expression and biological activities of the latter. Indeed, our studies addressing the above contexts support these implications and emphasize the complexity of the functional networks. Examination of expression of the physiological partners APC and hTid in untreated primary human colorectal cancers clearly showed that the expression of both tumor suppressors was altered in all investigated cases. The alterations detected concerned both the localization and the expression levels of the proteins addressed. Interestingly enough, the compartmentalization of both molecules in normal colon epithelium was lost with concomitant loss of

differentiation capacity of the tumors (Fig. 4; Table V). Since the molecular events leading to the colorectal cancers investigated are not known, speculations regarding the causality between a de-regulation of h*tid-1* and/or APC and the neoplastic transformation of these tumors cannot be made at the present state of knowledge. In the case of h*tid-1* gene products the altered expression involved all three splice variants in both cytosolic and mitochondrial location (Table II; Fig. 3). Since the Tid proteins participate in a spectrum of cellular functions, this finding implies that de-regulation of h*tid-1* may upset a variety of cellular processes. In view of the physiological link of APC-bound h*tid-1* with the components of the Hsp70 chaperone machinery, h*tid-1* alterations may also determine the proper function of this machinery and vice versa, its function may be altered by deregulation of Hsp70/Hsc70 molecules.

Collectively, our data describing the components of the multi-complex which includes hTid-bound APC and the proteins Hsp70/Hsc70 (22) and the expression study performed in a representative panel of colon cancers described in this study support our hypothesis that the interaction of hTid50/hTid48 with APC is associated with the APC-mediated Wg/Wnt function in morphogenetic processes signaling toward the cytoskeleton and cell polarity. Changes in the function(s) of one of the molecular partners may consequently result in alteration of the function(s) of the whole complex and, thus, in the de-regulation of these processes. Furthermore, since h*tid-1* seems to act upstream of APC, it can be expected that changes in the expression of the latter affect primarily the downstream components of the signaling. However, it should be considered that loss of APC will automatically lead to a collapse of the concentration gradient of the hTid proteins in the cell. Mutations in h*tid-1* on the other hand can directly affect both the function of APC and the functionally dependent down-stream components. Along this line a screen of colorectal tumors for h*tid-1* mutations may be helpful to establish its causal involvement in colorectal tumorigenesis and its role in APC-mediated functions. In view of the physiological link of APC-bound hTid50/hTid48 with the components of the Hsp70 chaperone machinery (22) and the correlation of alterations of h*tid-1* and Hsp70 expression with tumor progression, these data underline the causal importance of chaperones in cancer-related signaling.

Acknowledgements

This study was supported by the German Cancer Society (grant 10-1695-Ku2 to U. K.-D.) and the Italian Association of Cancer Research (grant to P.G. Natali).

References

1. Kurzik-Dumke U, Phannavong B, Gundacker D and Gateff E: Genetic, cytogenetic and developmental analysis of the *Drosophila melanogaster* tumor suppressor gene *lethal(2) tumorous imaginal discs* (*l(2)tid*). Differentiation 51: 91-104, 1992.
2. Kurzik-Dumke U, Gundacker D, Rentrop M and Gateff E: Tumor suppression in *Drosophila* is causally related to the function of the l*ethal(2)tumorous imaginal discs* gene, a dnaJ homolog. Dev Genet 16: 64-76, 1995.
3. Potter ChJ, Turenchalk GS and Xu T: *Drosophila* in cancer research. Trends Genet 16: 33-39, 2000.
4. Bryant PJ and Schmidt O: The genetic control of cell proliferation in *Drosophila* imaginal discs. J Cell Sci Suppl 13: 169-189, 1990.
5. Milán M: Cell cycle control in the *Drosophila* wing. BioEssays 20: 969-971, 1998.
6. Neumann CJ and Cohen SM: Long-range action of Wingless organizes the dorso-ventral axis of the *Drosophila* wing. Development 124: 871-880, 1997.
7. Chuang P-T and Kornberg TB: On the range of Hedgehog signaling. Curr Opin Genet Dev 10: 515-522, 2000.
8. Peifer M and Polakis P: Wnt signaling in oncogenesis and embryogenesis - a look outside the nucleus. Science 287: 1606-1609, 2000.
9. Taipale J and Beachy P: The Hedgehog and Wnt signaling pathways in cancer. Nature 17: 349-354, 2001.
10. Gateff E: Malignant neoplasms of genetic origin in the fruit fly *Drosophila melanogaster*. Science 200: 1446-1459, 1978.
11. Kurzik-Dumke U, Debes A, Kaymer M and Dienes P: Mitochondrial localization and temporal expression of the *Drosophila melanogaster* DnaJ homologous tumor suppressor Tid56. Cell Stress Chaperones 3: 12-27, 1998.
12. Canamasas I, Debes A, Natali PG and Kurzik-Dumke U: Understanding human cancer using *Drosophila*: Tid47, a cytosolic product of the DnaJ-like tumor suppressor gene *l(2)tid*, is a novel molecular partner of Patched related to skin cancer. J Biol Chem 278: 30952-30960, 2003.
13. Schilling B, De-Medina T, Syken J, Vidal M and Münger K: A novel human DnaJ protein, hTid-1 a human homolog of the *Drosophila* tumor suppressor protein Tid56, can interact with the human papillomavirus type 16 E7 oncoprotein. Virology 247: 74-85, 1998.
14. Sarkar S, Pollack BP, Lin K-T, Kotenko SV, Cook JR, Lewis S and Pestka S: HTid-1, a human DnaJ protein, modulates the interferon signalling pathway. J Biol Chem 276: 49034-49042, 2001.
15. Cheng H, Cenciarelli H, Shao Z, Vidal M, Parks WP, Pagano M and Cheng-Mayer C: Human T cell leukaemia virus type 1 Tax associates with a molecular chaperone complex containing hTid-1 and Hsp70. Curr Biol 11: 1771-1775, 2001.
16. Cheng H, Cenciarelli C, Tao M, Parks WP and Cheng-Mayer C: HTLV-1 Tax-associated hTId-1, a human DnaJ protein, is a repressor of IκB Kinase ß subunit. Biol Chem 277: 20605-20610, 2002.
17. Kim SW, Chao TH, Xiang R, Campbell MJ, Fearns C and Lee JD: Tid1, the human homologue of a *Drosophila* tumor suppressor, reduces the malignant activity of ErbB-2 in carcinoma cells. Cancer Res 64: 7732-7739, 2004.
18. Liu HY, MacDonald JIS, Hryciw T, Li CH and Meakin SO: Human Tid1 associates with TRK receptor tyrosine kinases and regulates neurite outgrowth in NNR5-TRKA cells. J Biol Chem 7: 19461-19471, 2005.
19. Bae MK, Jeong JW, Kim SH, Kim SY, Kang YJ, Kim DM, Bae SK, Yun I, Trentin GA, Rozakis-Adcock M and Kim KW: Tid-1 interacts with the von Hippel-Lindau protein and modulates angiogenesis by destabililzation of HIF-1α. Cancer Res 65: 2520-2525, 2005.
20. Trentin GA, Yin X, Tahir S, Lhotak S, Farhang-Fallah J, Li Y and Rozakis-Adcock M: A mouse homologue of the *Drosophila* tumor suppressor *l(2)tid* gene defines a novel Ras-GTPase-activating protein (RasGAP)-binding protein. J Biol Chem 276: 13087-13095, 2001.
21. Fujita M, Nagai Y, Sawada T and Heese K: Identification of rTid-1, the rat homologue of the *Drosophila* tumor suppressor *l(2)tid* gene. Mol Cell Biochem 258: 183-189, 2005.
22. Kurzik-Dumke U and Czaja J: H*tid-1*, the human homolog of the *Drosophila melanogaster l(2)tid* tumor suppressor, defines a novel physiological role of APC. Cell Signal 19: 1973-1985, 2007.
23. Yin X and Rozakis-Adcock M: Genomic organization and expression of the human *tumorous imaginal disc* (*TID1*) gene. Gene 278: 201-210, 2001.
24. Bienz M: APC: the plot thickens. Curr Opin Genet Dev 9: 595-603, 1999.
25. Arias AM, MC Brown A and Brennen K: Wnt signalling: pathway or network. Curr Opin Genet Dev 9: 447-454, 1999.
26. Bienz M and Clevers H: Linking colorectal cancer to Wnt signaling. Cell 103: 311-320, 2000.
27. Heppner Goss K and Groden J: Biology of the adenomatous polyposis coli tumor suppressor. J Clin Oncol 18: 1967-1979, 2000.
28. Fearnhead N, Britton MP and Bodmer WF: The ABC of APC. Hum Mol Genet 10: 721-733, 2001.

LH and Wittening CH: TNM Classification of Malignant
s. J. Willey-Liss, Willey Sons, Inc., New York, 2002.
30. Kinzler KW, Nilbert MC, Su L-K, Vogelstein B, Bryan TM, Levy DB, Smith KJ, Preisinger AC, Hedge P, McKechnie D, Finnier R, Markham A, Groffen J, Boguski MS, Altschul SF, Horii A, Ando H, Miyoshi Y, Miki Y, Nishisho I and Nakamura Y: Identification of FAP locus genes from chromosome 5q21. Science 253: 661-665, 1991.
31. Jackson P and Blythe D: Immunolabelling techniques for light microscopy. In: Immunochemistry. Beesleym JE (ed). IRL Press at Oxford University Press, Oxford, pp15-41, 1993.
32. Polakis P: The adenomatous polyposis coli (APC) tumor suppressor. Genes Dev 14: 1837-1851, 2000.
33. Sancho E, Batlle E and Clevers H: Signaling pathways in intestinal development and cancer. Annu Rev Cell Dev Cancer 20: 695-723, 2004.
34. Lambrechts A, Van Troys M and Ampe Ch: The actin cytoskeleton in normal and pathological cell motililty. Int J Biochem Cell Biol 36: 1890-1909, 2004.
35. Rassow J, Voos W and Pfanner N: Partner proteins determine multiple functions of Hsp70. Trends Cell Biol 5: 207-212, 1995.
36. Zuber U, Buchberger A, Laufen T and Bukkau B: DnaJ proteins. In: Molecular Chaperones in Life Cycle of Proteins. Fink AL and Goto Y (eds). Marcel Decker Inc., New York, pp241-271, 1998.
37. Ciocca DR and Calderwood SK: Heat shock proteins in cancer: diagnostic, prognostic, predictive and treatment implications. Cell Stress Chaperones 10: 86-103, 2005.
38. Laurent-Puig P, Blons H and Cugnenc PH: Sequence of molecular genetic events in colorectal tumorigenesis. Eur J Cancer Prev Suppl 1: 39-47, 1999.
39. Vogelstein B, Fearon ER, Hamilton SR, Kern SE, Preisinger AC, Leppert M, Nakamura Y, White R, Smits AM and Bos JL: Genetic alterations during colorectal tumor development. N Engl J Med 319: 525-532, 1999.
40. Kurzik-Dumke U, Schirmacher P, Bobkiewicz W, Kedzia H and Gozdzicka-Józefiak A: Preliminary study on expression of the human hTid protein, a homolog of the *Drosophila melanogaster* tumor suppressor Tid56 in various tumors. Cancer J 10: 56-61, 1997.